

Article

Hydrate Formation/Dissociation in (Natural Gas + Water + Diesel Oil) Emulsion Systems

Chang-Sheng Xiang ¹, Bao-Zi Peng ^{2,3}, Huang Liu ², Chang-Yu Sun ^{2,*}, Guang-Jin Chen ² and Bao-Jiang Sun ^{1,*}

¹ School of Petroleum Engineering, China University of Petroleum (Huadong), Qingdao 266580, China; E-Mail: xiangcs@acca21.org.cn

² State Key Laboratory of Heavy Oil Processing, China University of Petroleum, Beijing 102249, China; E-Mails: pbz1029@163.com (B.-Z.P.); mangliu5258@163.com (H.L.); gjchen@cup.edu.cn (G.-J.C.)

³ National Institute of Clean and Low-Carbon Energy, Beijing 102209, China

* Authors to whom correspondence should be addressed; E-Mails: cysun@cup.edu.cn (C.-Y.S.); sunbj@upc.edu.cn (B.-J.S.); Tel.: +86-10-89733156 (C.-Y.S.); Fax: +86-10-8973156 (C.-Y.S.).

Received: 11 December 2012; in revised form: 19 January 2013 / Accepted: 1 February 2013 /

Published: 18 February 2013

Abstract: Hydrate formation/dissociation of natural gas in (diesel oil + water) emulsion systems containing 3 wt% anti-agglomerant were performed for five water cuts: 5, 10, 15, 20, and 25 vol%. The natural gas solubilities in the emulsion systems were also examined. The experimental results showed that the solubility of natural gas in emulsion systems increases almost linearly with the increase of pressure, and decreases with the increase of water cut. There exists an initial slow hydrate formation stage for systems with lower water cut, while rapid hydrate formation takes place and the process of the gas-liquid dissolution equilibrium at higher water cut does not appear in the pressure curve. The gas consumption amount due to hydrate formation at high water cut is significantly higher than that at low water cut. Fractional distillation for natural gas components also exists during the hydrate formation process. The experiments on hydrate dissociation showed that the dissociation rate and the amount of dissociated gas increase with the increase of water cut. The variations of temperature in the process of natural gas hydrate formation and dissociation in emulsion systems were also examined.

Keywords: hydrate; emulsion; formation; dissociation; solubility

1. Introduction

Hydrate plugging often occurs in oil and gas multiphase flow pipelines, particularly in deepwater hydrocarbon exploration, development, and transportation. In general, thermodynamic inhibitors or low dosage hydrate inhibitors, such as kinetic inhibitors (KIs) and anti-agglomerants (AAs) [1–4], are injected to inhibit or control the formation of hydrates. On the other hand, hydrate slurry might become an alternative approach for oil and gas transportation, as large amounts of natural gas can be stored in the form of hydrates. This can both solve the flow assurance issues and reduce the cost of oil field development. Additionally, hydrate slurry flow also occurs in other applications based on gas hydrates, such as the continuous separation of gas mixtures via hydrate formation [5,6], refrigeration using hydrate slurries as a kind of cool storage material [7,8], *etc.* The characteristics of formation and dissociation of hydrate slurries is of importance for hydrate inhibition and corresponding applications.

The formation and dissociation of hydrates in pure water or porous media system are widely reported [9–12]. However, the situations in emulsion systems are somewhat different for that of pure water systems or porous media systems, where gas first needs to transfer through the oil phase and then reach the water surface to form a hydrate. Dalmazzone *et al.* [13] studied the methane hydrate dissociation equilibrium in water-in-oil emulsions using differential scanning calorimetry, and found that there are no measurable differences between bulk solutions and emulsions from a thermodynamic point of view. The hydrate formation in emulsions is related to the magnitude of the subcooling. Chen *et al.* [14] determined the metastable boundary conditions of water-in-oil emulsions in the methane hydrate formation region using a stepwise pressurization method. The experimental results showed that the metastable boundary pressures increase with decreasing water-droplet sizes, but when the system pressure exceeds the metastable boundary pressure, hydrate formation occurs and the metastable state of the emulsion collapses. Aichele *et al.* [15] used nuclear magnetic resonance to measure the formation of methane hydrates in water-in-oil emulsions and provided useful information regarding the relationship between drop size distributions and methane hydrate formation in emulsified systems. Boxall *et al.* [16] performed methane hydrate formation/dissociation experiments from water-in-oil emulsions with three different size distributions. The particle size distributions before and after hydrate formation showed that significant agglomeration occurred for the larger droplet sizes during the formation/dissociation of the hydrates. Irvin *et al.* [17] studied the mechanism of hydrate formation in water-in-oil microemulsions. Jakobsen *et al.* [18] studied the kinetics of trichlorofluoromethane hydrate formation in water-in-oil emulsions. In these studies on hydrate formation and dissociation in emulsions, methane was usually used as the hydrate-forming gas. This is not in accordance with the actual situation in multiphase flow pipelines where multi-component natural gas or condensate gas exists. The influence of oil-water ratio was also seldom examined in the literature. In addition, gas solubility in water-in-oil emulsions also influences the formation of hydrates. However, only the solubilities of pure gases or mixtures in pure water have been widely reported in the literature [19–22]. In this work, the solubilities of natural gas in water-in-oil emulsions were measured for different water cuts. The performance of the formation and dissociation of hydrate of emulsion systems were examined. The variations of temperature, pressure, and gas composition and amount during hydrate formation and dissociation were obtained for five water cuts.

2. Experimental

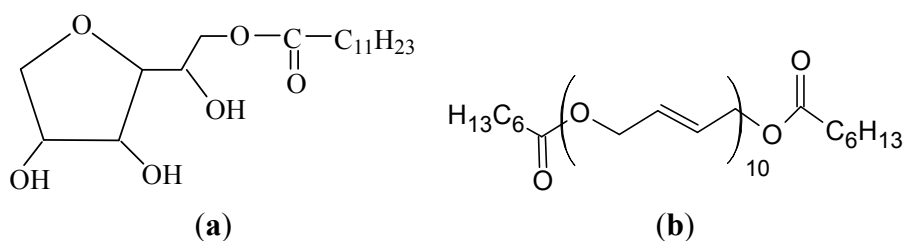
2.1. Materials

The natural gas used is the associated gas of an actual oil field, where the composition is: CO₂ 6.59, N₂ 18.46, CH₄ 72.03, C₂H₆ 0.63, C₃H₈ 0.63, i-C₄ 1.09, n-C₄ 0.27, and C₆ 0.30 mol%. Diesel oil with a freezing point of 263.2 K is adopted to mimic the actual fluid in deepwater pipelines. The composition of the diesel oil, which is measured through a simulated distillation method, is listed in Table 1. Double distilled water is used to form emulsions. A mixture of Span 20 and polyester polymer with a mixing ratio of 4:1 adopted as surfactant and anti-agglomerant were provided by Sinopharm Chemical Reagent Co. Ltd. (Beijing, China), and Henan Titaning Chemical Technology Co. Ltd. (Henan, China), respectively. The molecular structures of Span 20 and the polyester polymer are shown in Figure 1, where the molecular weights are 346 and 943, respectively. Additional information can be found in our previous work [23].

Table 1. Composition of the diesel oil used to form water-in-oil emulsion.

Component		mol%	wt%
C7	Heptanes	0.22	0.10
C8	Octanes	1.35	0.70
C9	Nonanes	3.60	2.09
C10	Decanes	3.70	2.39
C11	Undecanes	5.90	4.19
C12	Dodecanes	5.16	3.99
C13	Tridecanes	8.34	6.98
C14	Tetradecanes	13.60	12.25
C15	Pentadecanes	11.37	10.97
C16	Hexadecanes	10.08	10.37
C17	Heptadecanes	9.59	10.47
C18	Octadecanes	8.71	10.07
C20	Eicosanes	11.42	14.66
C24	Tetracosanes	6.81	10.47
C28+	Octacosanes plus	0.15	0.30
-	Total	100.00	100.00

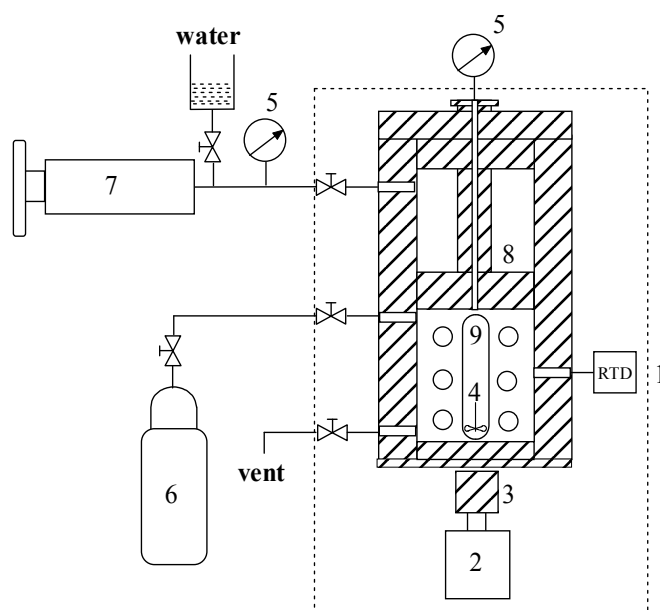
Figure 1. Molecular structure of anti-agglomerant used in this work: (a) Span 20; (b) esters polymer.



2.2. Apparatus and Procedures

A schematic diagram of the experimental apparatus used for solubility measurements and hydrate formation and dissociation studies is shown in Figure 2. It mainly consists of a high pressure reactor, a metering pump, a magnetic stirring system, and an air bath. The maximum volume of the high pressure reactor is 420 mL, with an operating pressure up to 20 MPa. A piston is installed in the reactor to adjust the volume and pressure of the fluid inside. There exists a window on the reactor and the morphology of the fluid can be observed from it. The operating temperature is measured by a Pt100 thermocouple and controlled by a Eurotherm temperature controller with an uncertainty of ± 0.1 K. The pressure gauge is calibrated using a standard RUSKA dead-weight pressure gauge with an uncertainty of $\pm 0.25\%$.

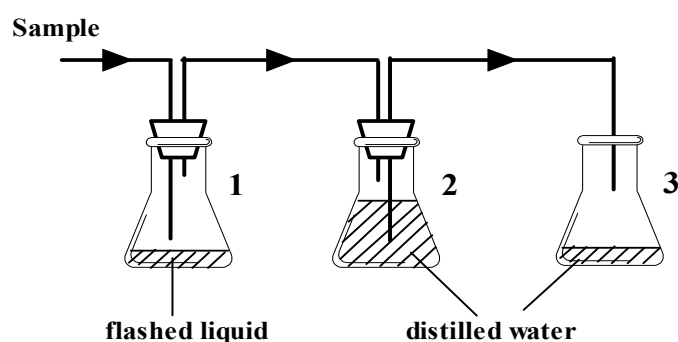
Figure 2. Schematic diagram of experimental apparatus used for solubility measurement and hydrate formation and dissociation study: 1. air bath; 2. motor; 3. magnet; 4. magnetic stirrer; 5. pressure gauge; 6. gas cylinder; 7. hand pump; 8. piston; 9. observation window; RTD: resistance thermocouple detector.



The experimental procedure for measuring the solubility of gas in emulsion is similar to our previous work and the accuracy of the experimental method has been verified from the solubility measurements of ethylene or methane in aqueous solutions of sodium dodecyl sulfate [24,25], which are described as follows: first, the whole experimental system was cleaned with petroleum ether and then flushed with hot distilled water, dried with pure nitrogen, and evacuated. Subsequently, about 200 mL of emulsion, prepared with a certain ratio of diesel oil and water by adding 3 wt% anti-agglomerant (Span 20 and polyester polymer with a mixing ratio of 4:1, based on water amount), was sucked into the reactor, which was then evacuated again to remove the air dissolved in the solution. The piston was pushed to the top of the reactor and the temperature of the air bath was then set to the specified value of 277.2 K. After the system temperature was stable, a certain amount of natural gas was charged into the reactor until the desired pressure was attained. Meanwhile, the stirrer

was started up with a constant stirring rate of 100 rpm. The natural gas was continuously charged into the reactor to balance the drop in the pressure due to the dissolution of natural gas in solution. When the system pressure was stable for more than 5 h, the gas—liquid dissolution equilibrium was assumed to be attained. After the equilibrium was reached, the stirrer was stopped and the reactor was kept static for at least 2 h to ensure that the natural gas bubbles would be completely separated from liquid. Thereafter, about 100 mL liquid was slowly charged to the sampling system under constant pressure maintained by pushing the piston in the reactor with the metering pump. The schematic diagram of the sampling system is shown in Figure 3. The collected liquid sample flashes in Flask 1 and the flashed gas displaces a portion of water filled in Flask 2 into Flask 3. The amounts of liquid in Flask 1 and Flask 3 were weighed, respectively. The volume of natural gas dissolved in solution is equal to the difference of volume between the liquid in Flask 3 and in Flask 1. The gas solubility was then calculated from the measured data above. It should be noted that the dissolution of gases in Flask 2 at atmospheric pressure was ignored in this work.

Figure 3. Schematic diagram of the liquid sampling system.



For the hydrate formation and dissociation in emulsion systems, the experimental procedure is as follows: first, the whole experimental system as shown in Figure 2 was cleaned as described above for the solubility measurements. Afterward, about 50 mL (diesel oil + water + 3 wt% anti-agglomerant) emulsion at a certain water cut was injected into the reactor, and the whole system was then evacuated. The temperature of the air bath was set to 277.2 K. After the system temperature was stable, natural gas was charged into the reactor until the pressure reached about 6.8 MPa. Then the stirrer was started up with a constant stirring rate of 100 rpm. Meanwhile, pressure and temperature in the reactor were recorded every certain time period. After the pressure in the system was stable at a constant value for 3 h, the formation of hydrate was assumed to be ended and then the dissociation of hydrate was started with the depressurizing method at a constant system volume [26]. That is, the vent was opened slowly and the system pressure decreased gradually until it reached a point somewhat above the equilibrium pressure of the natural gas hydrate at the present temperature. Afterward, the system was depressurized rapidly to atmospheric pressure. Soon after it attained 0.1 MPa, a water displacement system was started up to recover the gas released during the hydrate dissociation. The displaced water was weighed online using a precise electronic balance. Thereby, the accumulative volume of gas evolved in a certain time was obtained. The change of accumulative volume of gas evolved with time was then recorded.

3. Results and Discussion

3.1. Gas Solubility in Emulsion

It is known that gas solubility is related with the nucleation and growth of hydrates. Before the research on the kinetics of hydrate formation and dissociation of emulsion systems, it is necessary to obtain the gas solubility data under similar operation conditions. The solubilities of natural gas in emulsion systems were calculated by using the gas volume and liquid mass data obtained from the experimental procedure and method as described before. A mixture of Span 20 and polyester polymer with a mixing ratio of 4:1 is adopted to form water-in-oil emulsion and act as anti-agglomerant to prevent hydrate from agglomerating. The dosage of the anti-agglomerant is 3 wt%, based on the water mass in the solution. Five groups of water cuts were examined in this work, that is, 5, 10, 15, 20, and 25 vol%. The compositions of the natural gas and the diesel oil have been listed in the experimental section. To ensure that no hydrate forms during the experimental process for measuring the gas solubility, the experimental pressure should be lower than the equilibrium pressure value at the current temperature of 277.2 K. For a pure water environment, the phase equilibrium pressure of feed gas under 277.2 K is 1.36 MPa, according to the two-step hydrate formation mechanism [27]. The hydrate equilibrium pressure for emulsion systems is close to that of pure water system, although there exist higher metastable boundary conditions in water-in-oil emulsions [14]. The solubility results and the corresponding experimental conditions are listed in Table 2. From this Table, it can be seen that the experimental pressure is always lower than the hydrate equilibrium pressure, and it can be ensured that no formation of hydrate can occur. The gas solubility data at different water cuts and pressures are also shown in Figure 4.

Table 2. Natural gas solubilities in (diesel oil + water +3 wt% anti-agglomerant) emulsion systems at different pressures and water cuts at 277.2 K.

5 vol% water cut		10 vol% water cut		15 vol% water cut		20 vol% water cut		25 vol% water cut	
P (MPa)	s ($\times 10^3$)	P (MPa)	s ($\times 10^3$)	P (MPa)	s ($\times 10^3$)	P (MPa)	s ($\times 10^3$)	P (MPa)	s ($\times 10^3$)
0.2	16.68	0.2	12.20	0.5	12.25	0.3	5.43	0.2	3.16
0.4	24.15	0.5	18.12	0.8	18.25	0.6	9.30	0.4	5.13
0.8	35.65	0.8	25.29	1.0	22.35	0.9	13.39	0.8	10.21
1.2	46.86	1.2	35.69	1.2	25.59	1.2	17.93	1.2	15.42
-	-	1.35	39.59	1.35	28.92	1.35	20.56	-	-

From Figure 4, it can be found that when under a constant water cut, the solubility of natural gas in emulsion system increases almost linearly with the increase of pressure. As discussed for a (methane + octane) system [28], the surface excess concentration of natural gas on diesel oil increases with increasing pressure, where pressure has a positive effect for the adsorption of gas in diesel oil. However, when under a constant pressure, the solubility of gas in emulsions decreases with the increase of water cut. Figure 5 shows the natural gas solubility in (diesel oil + water + 3 wt% anti-agglomerant) emulsion at different water cuts when at the same pressure of 1.2 MPa.

Figure 4. Variation of solubilities of natural gas in (diesel oil + water + 3 wt% anti-agglomerant) emulsion systems with pressures and water cuts when at 277.2 K.

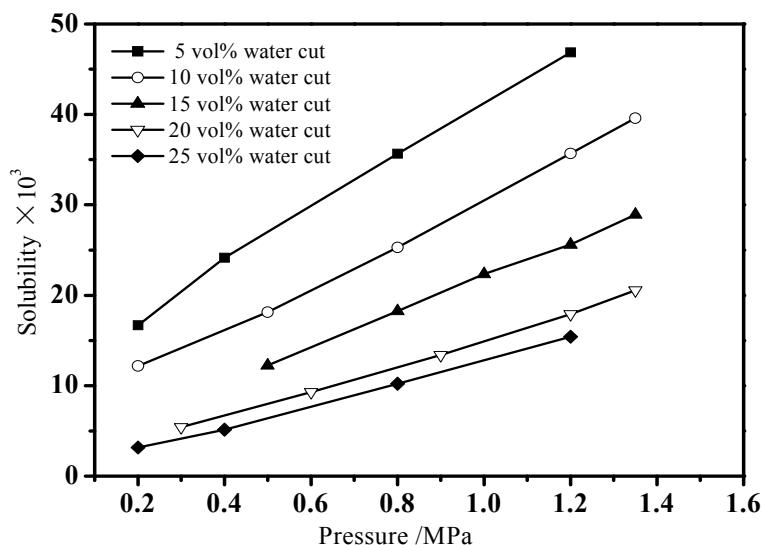
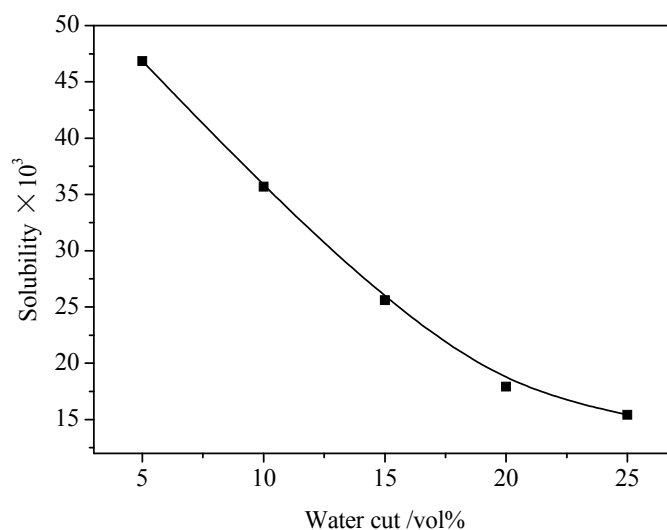


Figure 5. Variation of natural gas solubility in (diesel oil + water + 3 wt% anti-agglomerant) emulsion with water cuts when at 1.2 MPa.



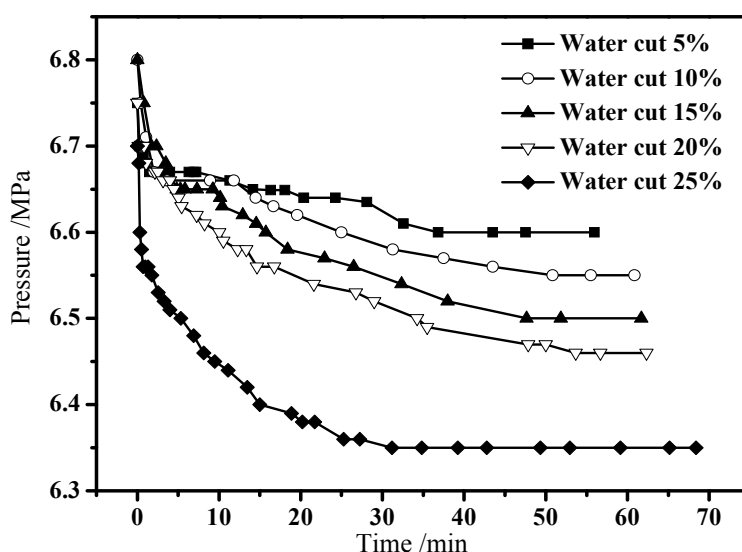
It can be seen that the magnitude of gas solubility in emulsions is mainly dependent on the fraction of the oil phase. The adsorption of natural gas on diesel oil is higher than that on water. The intermolecular interaction between natural gas molecules and nonpolar liquid weakens at higher pressures, and is lower than that between gas molecules and polar liquid. There also exists the surfactant fractionation between the oil phase and water phase, with which more ratio of surfactant will be in the oil phase. In addition, it can be found that the gas solubility in the emulsion decreases more rapidly with the increase of water cut when at lower water cut, while the gas solubility curve becomes flat with the continuous increase of water cut. When at a lower water cut, the formed emulsion is easily dispersed into the oil phase and water phase in a short time, and the gas solubility in the liquid phase is chiefly influenced by the oil phase fraction in the solution. Under higher water cut, a more stable emulsion will form and gas solubility is chiefly influenced by the type of the emulsion. The addition of

the anti-agglomerant is also beneficial to the improvement of gas solubility in the oil-water solutions. Oil and water will be adequately emulsified after adding the suitable amount of the anti-agglomerant and the solution tends to be more hydrophobic. Meanwhile, there exists adsorption for gas molecular by the anti-agglomerant in the liquid phase, which will result in the increase of the gas solubility in the emulsion compared with a situation with no surfactant system.

3.2. Hydrate Formation in Emulsion Systems

The performance of hydrate formation and dissociation in emulsion systems is essential for natural gas transportation in the form of hydrate slurry. It is also of importance to solve the hydrate plugging issue in pipelines and devices. In this work, according to the procedure described in Section 2, we performed hydrate formation experiments for (diesel oil + water + 3 wt% anti-agglomerant) systems at five different water cuts, 5, 10, 15, 20, and 25 vol%. The system volume is kept constant while the system pressure will decrease due to the dissolution of gas and the formation of hydrate. The initial pressure and temperature of the systems for the five water cuts are all specified at about 6.8 MPa and 277.2 K. Natural gas listed in Section 2 is used as feed gas. Figure 6 shows the variations of the system pressure with the elapsed time during the hydrate formation process for the different water cuts.

Figure 6. Variation of pressure with time in the process of natural gas hydrate formation in emulsions.

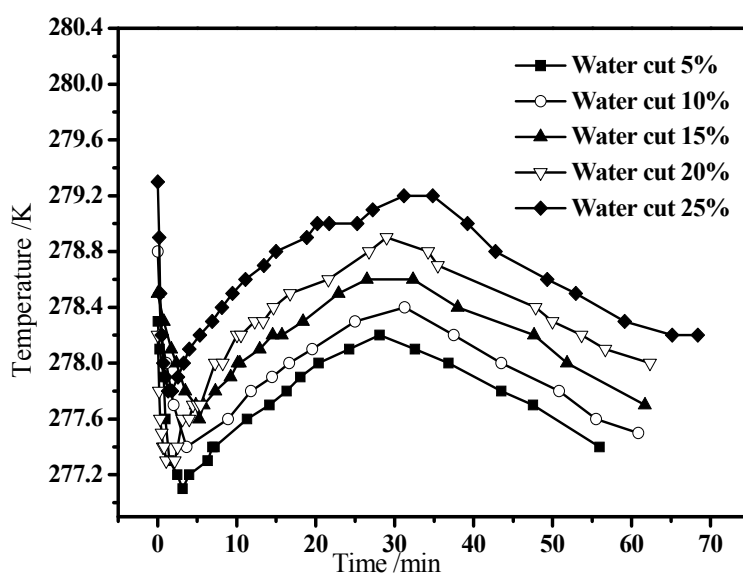


It can be found that when at a low water cut, the system pressure decreases rapidly in the initial stage due to the dissolution of natural gas in the emulsion, and then the decrease of pressure tends to be steady while a large amount of formation of hydrate is not obvious for a certain time. Thereafter, hydrate forms apparently and the system pressure decreases gradually until the end of hydrate formation. From Figure 6, it can be seen that there exists the slow formation stage for systems with water cuts of 5, 10, and 15 vol%. The duration of this stage reduces with the increase of the water cut. For the systems with high water cut, such as 20 and 25 vol%, the gas dissolution and rapid hydrate formation are taking place almost at the same time. Under high water cut conditions, the influence of dissolution on the extent of the decrease of heavy components in natural gas is low compared with low

water cut systems. This will result in the large driving force for hydrate nucleation for high water cut systems. From a comparison of the variation of system pressure at five different water cuts, the gas consumption due to the hydrate formation at high water cut is significantly higher than that at low water cut. As the gas solubility at high water cut is even lower than that at low water cut as shown in Figure 4, the decrease of the system pressure is largely derived from the formation of hydrate.

Figure 7 shows the variations of the temperature in the reactor with the elapsed time at different water cuts during the hydrate formation process. In the beginning, the natural gas injected into the reactor is under the same room temperature, which is higher than the temperature specified in the reactor. There exists different heat of solution of the feed natural gas for different water cut systems. Therefore, at the initial stage, the system temperature is a little higher than 277.2 K and some different for the different water cut systems. It decreases to be close to the specified value with the action of the temperature control by the air bath. With the decrease of the system temperature, an inflexion of the experimental temperature curve appears and it changes to an increase because of the exothermic reaction induced from the large amount of hydrate formation. It can be found that the time of appearance of the inflexion at different water cuts is different. It is related to the synergistic heat effect provided by the constant-temperature air bath, hydrate formation amount, and heat of solution of the feed natural gas for different water cut systems. Meanwhile, the temperature value at the inflexion with higher water cut is higher. After the inflexion, the system temperature continues increasing with the continuous formation of hydrate until it attains a maximum value for every water cut, as shown in Figure 7. Thereafter, with the reduction of formation of hydrate, the system temperature decreases gradually toward the specified value of the air bath. It can be seen that the maximum value of the system temperature for five water cuts increases with the increase of the water cut, showing that there exists a certain relationship between the amount of hydrate formed and the water cut.

Figure 7. Variation of temperature with time in the process of natural gas hydrate formation in emulsions.



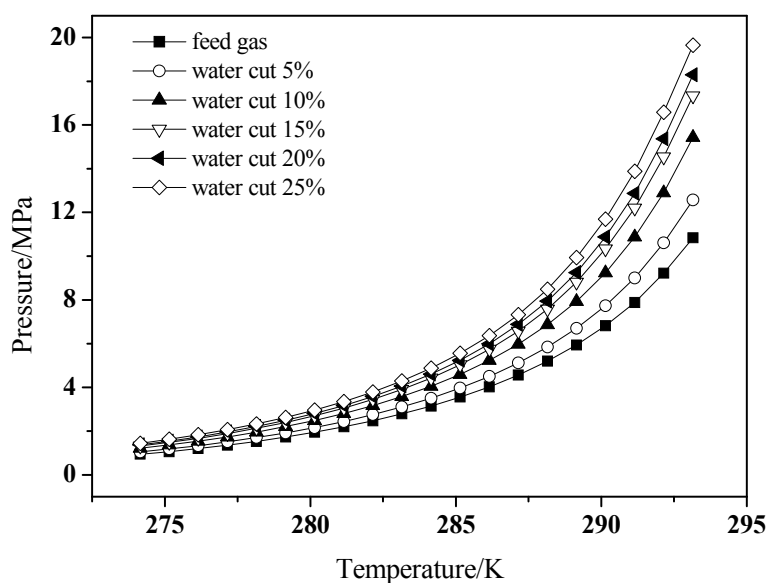
It should be noticed that the composition of the gas phase changes with the dissolution of gas in the emulsion and especially the formation of hydrate. The compositions of equilibrium gas at the end of

hydrate formation are also different for different water cuts, which will result in variations of the hydrate formation pressures under equilibrium conditions. The analysis of the natural gas composition after the end of hydrate formation for five water cuts shows that, compared with the initial feed gas, the total content of N_2 and CH_4 in equilibrium gas in general increases with the increase of water cut, while the total content of heavy components such as C_2H_6 , C_3H_8 , and C_4H_{10} decreases with the increase of water cut. There exists a fractional distillation for light and heavy gas components during hydrate formation and gas dissolution [29]. The mole compositions for the equilibrium gas at different water cuts are listed in Table 3 and the equilibrium conditions for hydrate formation calculated by hydrate thermodynamic model base on two-step mechanism [27] are shown in Figure 8. It can be found that the hydrate formation pressure for the equilibrium gas also increases with the increase of water cut.

Table 3. Composition of equilibrium gases at different water cuts.

Water cut	Fraction (mol%)							
	CO_2	N_2	CH_4	C_2H_6	C_3H_8	i-C4	n-C4	C6
5 wt%	6.51	18.56	72.63	0.51	0.49	0.81	0.24	0.25
10 wt%	6.28	18.99	73.17	0.33	0.25	0.59	0.19	0.19
15 wt%	6.15	19.24	73.42	0.25	0.18	0.48	0.14	0.14
20 wt%	6.06	19.28	73.59	0.22	0.15	0.44	0.14	0.12
25 wt%	5.87	19.32	73.83	0.19	0.15	0.44	0.13	0.07

Figure 8. Hydrate formation condition of equilibrium gases for different water cuts.



3.3. Hydrate Dissociation in Emulsion Systems

After the end of the hydrate formation stage, it was dissociated by the depressurizing method at a constant system volume for hydrate formed from (diesel oil + water + 3 wt% anti-agglomerant) systems at different water cuts, 5, 10, 15, 20, and 25 vol%, respectively. Figure 9 shows the variation of the amount of decomposed gas with time in the process of natural gas hydrate dissociation in emulsions at five different water cuts. It can be found that the amount of gas dissociated increases with

the increase of water cut, which also corresponds to the amount of gas consumption during the hydrate formation stage. A longer time is needed for thorough dissociation of hydrate at a higher water cut compared with the system at a low water cut. From the slope of the curve of dissociated gas amount with the elapsed time, it can be found that the dissociation rate at high water cut is significantly larger than that at low water cut when within the same dissociation time. For oil-water emulsion systems with a certain surfactant, the formed hydrate is usually in the form of slurry. The dissociation of hydrate slurry is comparatively uniform compared with the block hydrate. The gas amount dissociated for high water cut system is therefore larger than that for low water cut system when within the same time period.

Figure 9. Variation of the quantity of decomposed gases with time in the process of natural gas hydrate dissociation in emulsions.

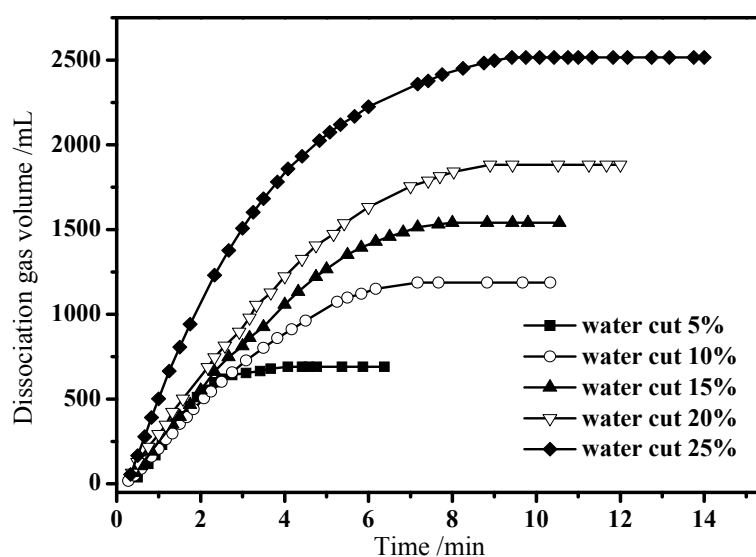
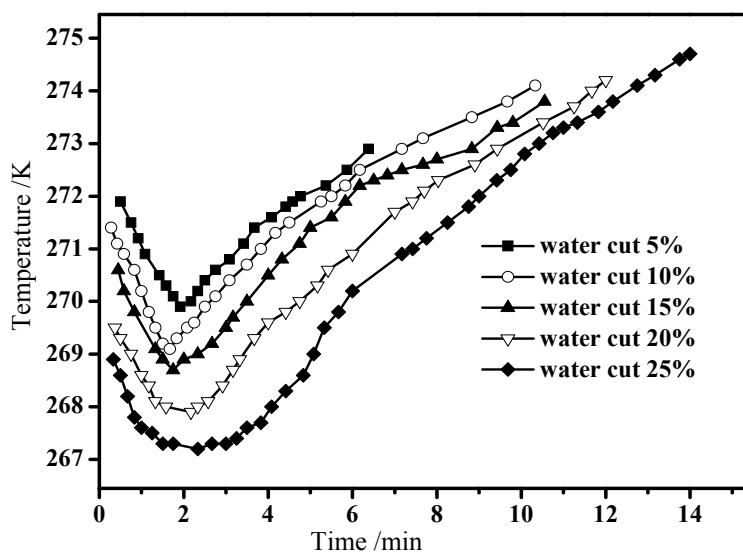


Figure 10 shows the variation of temperature in the process of gas hydrate dissociation in emulsion systems at five different water cuts. In the first stage of the natural gas hydrate dissociation experiments, the system pressure decreases gradually to attain a pressure value a little higher than the equilibrium pressure and then was depressurized rapidly to 0.1 MPa. The dissociation of hydrate and the throttling effect of rapidly depressurization will induce the decrease of temperature of the hydrate-containing slurry. It can be seen that the temperature at the beginning of the hydrate dissociation is lower than the specified value of the air bath as shown in Figure 10. Afterward, with the continuous dissociation of hydrate, the system temperature decreases gradually to be a much lower value due to the endothermal effect of hydrate dissociation. With the decrease of dissociation rate and amount of undecomposed hydrate, the system temperature begins to rise with the synergistic heat effect provided by the constant-temperature air bath and hydrate dissociation. It can be found that the time which the temperature starts to rise is later for higher water cut because of the higher amount of hydrate formed at higher water cut. In addition, as shown in Figure 10, the decrease extent of the temperature in the initial stage increases with the increase of water cut in the emulsion, which also resulting from the high amount of hydrate and high dissociation rate for high water cut systems.

Figure 10. Variation of temperature in the process of natural gas hydrate dissociation in emulsions.



4. Conclusions

The solubility and hydrate formation/dissociation of natural gas in (diesel oil + water + 3 wt% anti-agglomerant) emulsion systems were studied at five water cuts. The experimental results show that the solubility of natural gas in emulsion system increases almost linearly with the increase of pressure, while it decreases with the increase of water cut. There exists an initial slow hydrate formation stage for systems with water cuts of 5, 10, and 15 vol%, while rapid hydrate formation is taking place and the process of the gas-liquid dissolution equilibrium at 20 and 25 vol% does not appear in the pressure curve. The gas consumption due to the hydrate formation at high water cut is significantly higher than that at low water cut. For hydrate dissociation processes, the amount of gas dissociated increases with the increase of water cut. The dissociation rate at high water cut is significantly larger than that at low water cut for the same dissociation time. The variation of the temperature during the formation and dissociation of hydrate is related to the synergistic heat effect of exothermic/endothermal effect of phase transition, the throttling effect of depressurization, and heat transfer by the environment.

Acknowledgments

The financial supports received from the National Science & Technology Major Project (No. 2011ZX05026-004) are gratefully acknowledged.

References

- Huo, Z.; Freer, E.; Lamar, M.; Sannigrahi, B.; Knauss, D.M.; Sloan, E.D. Hydrate plug prevention by anti-agglomeration. *Chem. Eng. Sci.* **2001**, *56*, 4979–4991.
- Arjmandi, M.; Tohidi, G.; Danesh, A.; Todd, A.C. Is subcooling the right driving force for testing low-dosage hydrate inhibitors. *Chem. Eng. Sci.* **2005**, *60*, 1313–1321.

3. Zanota, M.L.; Dicharry, C.; Graciaa, A. Hydrate plug prevention by quaternary ammonium. *Energy Fuels* **2005**, *19*, 584–590.
4. Kelland, M.A. History of the development of low dosage hydrate inhibitors. *Energy Fuels* **2006**, *20*, 825–847.
5. Zhang, L.W.; Chen, G.J.; Sun, C.Y.; Fan, S.S.; Ding, Y.M.; Wang, X.L.; Yang, L.Y. The partition coefficients of ethylene between hydrate and vapor for methane + ethylene + water and methane + ethylene + SDS + water system. *Chem. Eng. Sci.* **2005**, *60*, 5356–5362.
6. Sun, C.Y.; Ma, C.F.; Chen, G.J.; Zhang, S.X. Experimental and simulation of single equilibrium stage separation of (methane + hydrogen) mixtures via forming hydrate. *Fluid Phase Equilib.* **2007**, *261*, 85–91.
7. Marinha, S.; Delahaye, A.; Fournaison, L. Solid fraction modeling for CO₂ and CO₂-THF hydrate slurries used as secondary refrigerants. *Int. J. Refrig.* **2007**, *30*, 758–766.
8. Wang, W.C.; Fan, S.S.; Liang, D.Q.; Yang, X.Y. Experimental study on flow characters of CH₃CCl₂F hydrate slurry. *Int. J. Refrig.* **2008**, *31*, 371–378.
9. Zhao, J.F.; Cheng, C.X.; Song, Y.C.; Liu, W.G.; Liu, Y.; Xue, K.H.; Zhu, Z.H.; Yang, Z.; Wang, D.Y.; Yang, M.J. Heat transfer analysis of methane hydrate sediment dissociation in a closed reactor by a thermal method. *Energies* **2012**, *5*, 1292–1308.
10. Xiong, L.J.; Li, X.S.; Wang, Y.; Xu, C.G. Experimental study on methane hydrate dissociation by depressurization in porous sediments. *Energies* **2012**, *5*, 518–530.
11. Horvat, K.; Kerkar, P.; Jones, K.; Mahajan, D. Kinetics of the formation and dissociation of gas hydrates from CO₂-CH₄ mixtures. *Energies* **2012**, *5*, 2248–2262.
12. Sun, C.Y.; Chen, G.J. Methane hydrate dissociation above 0 °C and below 0 °C. *Fluid Phase Equilib.* **2006**, *242*, 123–128.
13. Dalmazzone, D.; Kharrat, M.; Lachet, V.; Fouconnier, B.; Clause, D. DSC and PVT measurements: Methane and trichlorofluoromethane hydrate dissociation equilibria. *J. Therm. Anal. Calorim.* **2002**, *70*, 493–505.
14. Chen, J.; Sun, C.Y.; Liu, B.; Peng, B.Z.; Wang, X.L.; Chen, G.J.; Zuo, J.Y.; Ng, H.J. Metastable boundary conditions of water-in-oil emulsions in the hydrate formation region. *AIChE J.* **2012**, *58*, 2216–2225.
15. Aichele, C.P.; Chapman, W.G.; Rhyne, L.D.; Subramani, H.J.; Montesi, A.; Creek, J.L.; House, W. Nuclear Magnetic Resonance analysis of methane hydrate formation in water-in-oil emulsions. *Energy Fuels* **2009**, *23*, 835–841.
16. Boxall, J.; Greaves, D.; Mulligan, J.; Koh, C.; Sloan, E.D. Gas hydrate formation and dissociation from water-in-oil emulsions studied using PVM and FBRM particle size analysis. In *Proceedings of the 6th International Conference on Gas Hydrate*, Vancouver, Canada, 6–10 July 2008.
17. Irvin, G.; Li, S.; Simmons, B.; John, V.; Mcpherson, G.; Max, M.; Pellenbarg, R. Control of gas hydrate formation using surfactant systems: Underlying concepts and new applications. *Ann. N. Y. Acad. Sci.* **2000**, *912*, 515–526.
18. Jakobsen, T.; Sjobom, J.; Ruoff, P. Kinetics of gas hydrate formation in w/o emulsions. *Colloids Surf. A Physicochem. Eng. Asp.* **1996**, *112*, 73–84.
19. Lekvam, K.; Bishnoi, P.R. Dissolution of methane in water at low temperatures and intermediate pressures. *Fluid Phase Equilib.* **1997**, *131*, 297–309.

20. Chapoy, A.; Mokraoui, S.; Valtz, A.; Richon, D.; Mohammadi, A.H.; Tohidi, B. Solubility measurement and modeling for the system propane-water from 277.62 to 368.16 °C. *Fluid Phase Equilib.* **2004**, *226*, 213–220.
21. Someya, S.; Bando, S.; Chen, B.; Song, Y.; Nishio, M. Measurement of CO₂ solubility in pure water and the pressure effect on it in the presence of clathrate hydrate. *Int. J. Heat Mass Transf.* **2005**, *48*, 2503–2507.
22. Wang, L.K.; Chen, G.J.; Han, G.H.; Guo, X.Q.; Guo, T.M. Experimental study on the solubility of natural gas components in water with or without hydrate inhibitor. *Fluid Phase Equilib.* **2003**, *207*, 143–154.
23. Peng, B.Z.; Chen, J.; Sun, C.Y.; Dandekar, A.; Guo, S.H.; Liu, B.; Mu, L.; Yang, L.Y.; Li, W.Z.; Chen, G.J. Flow characteristics and morphology of hydrate slurry formed from (natural gas + diesel oil/condensate oil + water) system containing anti-agglomerant. *Chem. Eng. Sci.* **2012**, *84*, 333–344.
24. Luo, H.; Sun, C.Y.; Peng, B.Z.; Chen, G.J. Solubility of ethylene in aqueous solution of sodium dodecyl sulfate at ambient temperature and near the hydrate formation region. *J. Colloid Interf. Sci.* **2006**, *298*, 952–956.
25. Peng, B.Z.; Chen, G.J.; Luo, H.; Sun, C.Y. Solubility measurement of methane in aqueous solution of sodium dodecyl sulfate at ambient temperature and near hydrate conditions. *J. Colloid Interf. Sci.* **2006**, *304*, 558–561.
26. Lin, W.; Chen, G.J.; Sun, C.Y.; Guo, X.Q.; Wu, Z.K.; Liang, M.Y.; Chen, L.T.; Yang, L.Y. Effect of surfactant on the formation and dissociation kinetic behavior of methane hydrate. *Chem. Eng. Sci.* **2004**, *59*, 4449–4455.
27. Chen, G.J.; Guo, T.M. A new approach to gas hydrate modeling. *Chem. Eng. J.* **1998**, *71*, 145–151.
28. Peng, B.Z.; Sun, C.Y.; Liu, B.; Zhang, Q.; Chen, J.; Li, W.Z.; Chen, G.J. Interfacial tension between methane and octane at elevated pressure at five temperatures from (274.2 to 282.2) K. *J. Chem. Eng. Data* **2011**, *56*, 4623–4626.
29. Tang, X.L.; Jiang, Z.X.; Li, F.G.; Sun, C.Y.; Chen, G.J. Solubility measurement of natural gas in reservoir formation water under (333.2 to 393.2) K and (15.0 to 43.6) MPa. *J. Chem. Eng. Data* **2011**, *56*, 1025–1029.